Available online at www.sciencedirect.com
ScienceDirect
Progress in Natural Science 19 (2009) 615–621
Progress in Natural Science
www.elsevier.com/locate/pnsc

Effects of disinhibition on spatiotemporal pattern of neuronal first recruitment in neuronal networks

Liangbin Pan [a,b,c,1], Xindong Song [a,b,c,1], Guangxin Xiang [a,b,c], Jing Zhu [a,b,c], Jing Cheng [a,b,c,d,*]

[a] *Medical Systems Biology Research Center, Tsinghua University School of Medicine, Beijing 100084, China*
[b] *Department of Biological Sciences and Biotechnology, Tsinghua University, Beijing 100084, China*
[c] *National Engineering Research Center for Beijing Biochip Technology, 18 Life Science Parkway, Beijing 102206, China*
[d] *State Key Laboratory of Biomembrane and Membrane Biotechnology, Tsinghua University, Beijing 100084, China*

Received 19 May 2008; received in revised form 2 July 2008; accepted 2 July 2008

Abstract

The propagation of neuronal activities is a key feature to understanding information processing in networks. The analysis based on first-spikes of bursts in turn plays an important role in the research of neuronal activity propagation. Our focus here is to investigate how spatiotemporal patterns of neuronal first-spikes are affected by disinhibition. Multi-electrode arrays were used to record stimulation-evoked bursts of multiple neurons in randomly cultured neuronal networks. Both the precise timing of and the rank relationships between first-spikes were analyzed. Compared with evoked bursts in the network's native state, the precise first-spike latencies in its disinhibited state are more consistent and the propagation of its bursting activities is much faster. Additional points of interest are that disinhibited neuronal networks can be evoked to generate stable and distinguishable neuronal first recruitment spatiotemporal patterns specific to the stimulation site, and that the disinhibition may cause the original spatiotemporal patterns to change in a heterogeneous manner with regards to different propagation pathways.

Keywords: Neuronal recruitment; Spatiotemporal pattern; Disinhibition; Network; Multi-electrode array

1. Introduction

In a neuronal network containing both excitatory and inhibitory synapses, the study of spatiotemporal patterns of neuronal activities provides a global view on network behavior, and is a key method for understanding the propagation of neuronal activities in a network in both experimental and theoretical investigations [1–9]. There have been *in vitro* experiments conducted to investigate how the blockade of inhibitory synapses influences neuronal activities on the network level using simultaneous multiple neuron recordings [10–12]. There have also been previous efforts to characterize bursting in disinhibited networks based on spatiotemporal patterns [1,3,7]. However, studies that focused on spatiotemporal patterns of spontaneous neural activities had more ambiguous data compared to those that focused on electrically stimulated activities. Those that had focused on electrically stimulated activities in turn failed to record and represent their data in a clear and precise fashion.

In this study, we aimed to examine the spatiotemporal patterns of neuronal recruitment in disinhibited networks and to reveal the effects of disinhibition on a configuring pathway during the propagation of the burst evoked by

* Corresponding author. Tel: +86 10 62772239; fax: +86 10 80726898.
E-mail address: jcheng@tsinghua.edu.cn (J. Cheng).
[1] These authors contributed equally to this work.

1002-0071/$ - see front matter © 2009 National Natural Science Foundation of China and Chinese Academy of Sciences. Published by Elsevier Limited and Science in China Press. All rights reserved.
doi:10.1016/j.pnsc.2008.07.019

an electrical stimulation. The multi-electrode array (MEA) technique was used to record synchronous bursting activities from multiple neurons in cultured neuronal networks. The first-spike times in bursting activities reflect the order of neuronal first recruitment, which in turn says something about the order of propagation in a neuronal pathway. To represent the spatiotemporal patterns of neuronal first engagement, we compared the first-spike timings between every pair of neurons in a burst and identified the rank relationships between them. To study the effect of inhibition on the dynamics of first-spike latencies, we performed return plot analysis on precise first-spike latencies of individual neurons in successive bursts.

2. Materials and methods

2.1. MEA and cell culture

The multi-electrode arrays (MEAs) were fabricated on polished Pyrex glass wafers (Corning Incorporated, Corning, USA). Each array consisted of 96 Au/Ti electrodes, which were 30 μm in diameter and spaced 200 μm away from one another. MEAs were flexibly encapsulated on printed circuit boards, and the electrodes were platinized (Fig. 1(a) and (b)) (CapitalBio, Beijing, China). For more information please refer to [13].

In this experiment, we adhered to the animal welfare guidelines elaborated in the National Institutes of Health (NIH) guide for the care and use of laboratory animals. Neocortical neurons were obtained from the brains of embryonic day 18 Sprague–Dawley rats. All efforts were made to reduce the number of animals used and to minimize animal suffering. Neocortical tissue was mechanically dissociated under sterile conditions and enzymatically digested. Cells were separated in the culture medium containing 47% MEM (Invitrogen), 47% Neurobasal^{TM} medium with B27 (Invitrogen), 5% FBS and 0.5 mM Glutamax (Invitrogen), and 100,000 cells in 200 μl of culture medium were plated on poly-L-lysine (Sigma, Saint Louis, MO) and laminin (Sigma)-coated MEAs and formed a monolayer of cells with a density of 2000 cells per square millimeter. Cultures were maintained in a tissue incubator at 37 °C with an atmosphere consisting of 5% CO_2, 95% air, and at 100% relative humidity. Half of the volume of culture medium was replaced twice every week. Fig. 1(c) shows a network of cortical neurons cultured on an MEA.

2.2. Electrical stimulation and multichannel extracellular signal recording

Electrical stimuli were generated by an electrical stimulator (A310 accupulser, WPI, Sarasota, FL). Electrical pulses (1 V, 250 μs pulse width) were applied. Three electrodes, each located in a corner of the electrode grid layout, were chosen to be the stimulation sites, and are represented by S1, S2 and S3, respectively. At any point in time, only one of the three stimulation sites was used to transfer the electrical pulses. Electrical pulses were applied between the chosen stimulation site and a reference electrode, a Ag/AgCl wire immersed in culture medium (Fig. 1(d)).

A multichannel neural signal amplifier (Cyberkinetics, Salt Lake City, UT) with a frequency range of 250–7500 Hz and a gain of 5000× was used. Signals were sampled at a frequency of 30 kilosample/s using a neural signal acquisition system (Cyberkinetics). Before the experiments, thresholds (5-fold rms noise) were defined separately for all recording channels. Prior to the analysis of the acquired data, a spike-sorting algorithm [14] was used to minimize data ambiguity in the event that different neural spike sources were recorded by the same electrode. Fig. 1(e) and (f) show examples of evoked bursts in the native state and evoked bursts in the disinhibited state, respectively. The stimulus artifacts persisted for several milliseconds, and were followed by a distinct silent period of 5–40 ms before the onset of the actual bursting response. As such, stimulation and the resultant bursting can be clearly distinguished, and we were able to determine the timings of first-spikes of stimuli-evoked synchronous bursting.

During the stimulation and recording, the cultured networks were maintained in a tissue incubator at 37 °C with an atmosphere consisting of 5% CO_2, 95% air and at 100% relative humidity.

2.3. Application of antagonists of inhibitory synapses

To investigate the effects of disinhibition on spatiotemporal relationships among neurons, inhibitory synaptic blockers, i.e., bicuculline (BIC, 20 μM) (Sigma), CGP35348 (1 μM) (Sigma) and strychnine (STR, 1 μM) (Sigma), were applied to block $GABA_A$, $GABA_B$ and Gly receptors, respectively.

2.4. The experimental procedure

The experiments were performed in the third week after plating. There are two steps in each experiment: (1) Perform six recording sessions (RSs) by activating each of the predetermined stimulation sites twice in the following sequence: S1, S2, S3, and then S1, S2, S3, with each RS containing about 40 evoked bursts; (2) add the antagonists to the cell culture medium and repeat step (1) in the presence of the antagonists. The same experimental procedure was performed on five different neuronal networks separately.

2.5. Data analysis

We defined the latency of the first-spike as the interval between the onset of the first-spike and the starting time of the electrical pulse immediately before. We performed return plot analysis on the latencies of first-spikes of individual neurons in successive bursts. Return plots elucidate a temporal relationship of the first-spikes between succes-

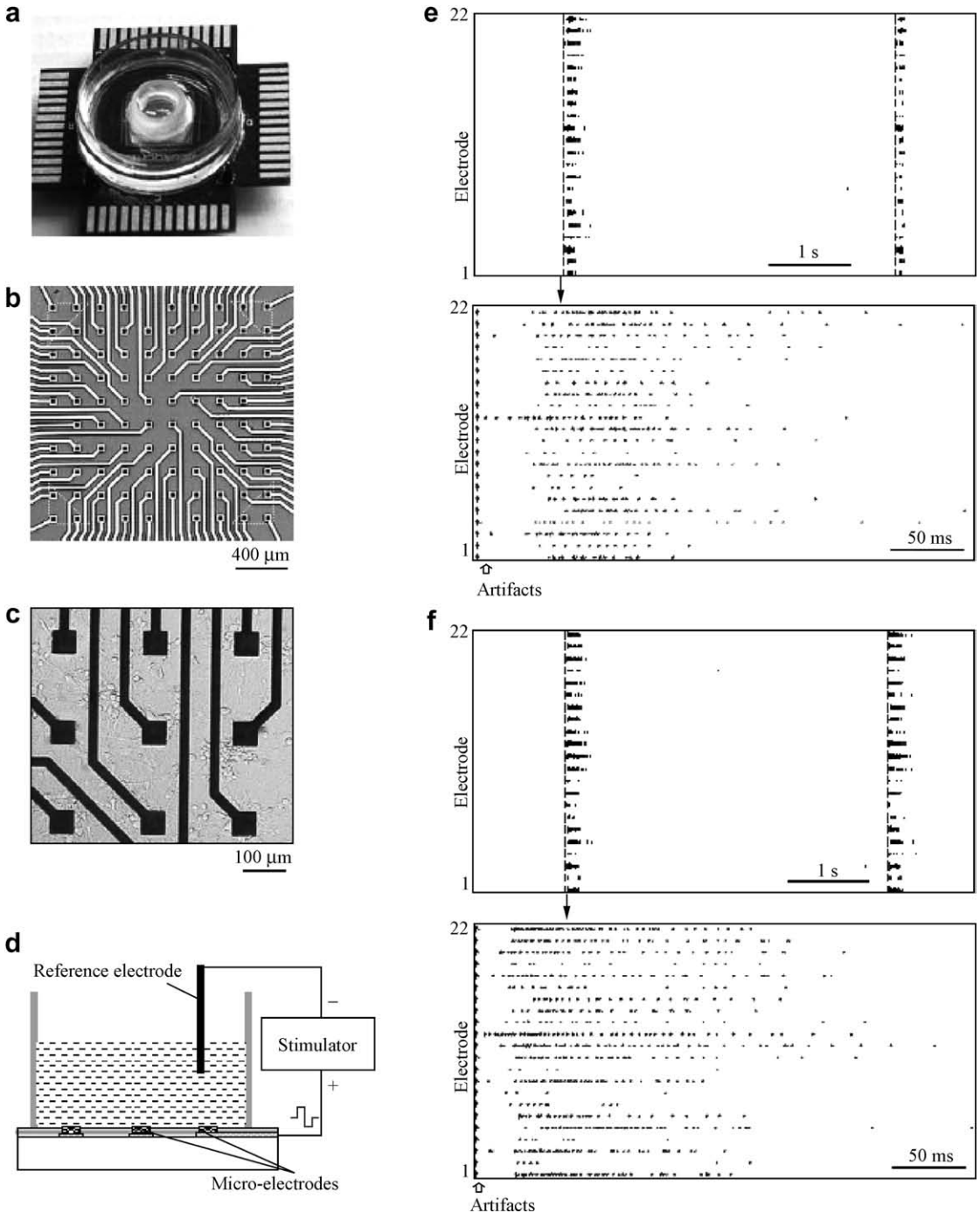

Fig. 1. Experimental setup and signal recording. (a) An MEA encapsulated on a printed circuit board; (b) an array of 96 micro-electrodes; (c) a network of cortical neurons cultured on an MEA; (d) stimulation setup. The biphasic electrical pulses were applied between a micro-electrode on the MEA and a reference electrode (Ag/AgCl wire) suspended in culture medium; (e) two evoked bursts simultaneously recorded by 22 electrodes from a network in its native state. The extracted sections from a burst show the details of both artifacts and spikes; (f) two evoked bursts simultaneously recorded by 22 electrodes from a network in its disinhibited state. The extracted sections from a burst show the details of both artifacts and spikes.

sive bursts, by recursively plotting the first-spike latency of the kth burst against the first-spike latency of the k+1st. The appearance of clusters in return plots reflects a conserved temporal pattern in successive bursts, and the spread of clusters reflects the precision of first-spike conservation.

Furthermore, an analysis method based on the rank relationship between the first-spikes was performed. For all the bursts in a recording session (RS), let the number of recorded units be N. For RS k ($k = 1,2,\ldots,M$), and for a pair of units (i and j) ($i, j = 1,2,\ldots,N$), let the percentage of the bursts in which the first-spike of unit i firing ahead of

that of unit j in the RS be p^0_{kij} (0–1), so matrix P^0_k is obtained.

$$P^0_k = \begin{pmatrix} p^0_{k11} & \cdots & p^0_{k1N} \\ \vdots & \ddots & \vdots \\ & p^0_{kij} & \\ p^0_{kN1} & \cdots & p^0_{kNN} \end{pmatrix}, \quad (k = 1, ..., M)$$

Matrix P^0_k was defined as the rank-probability-matrix (RPM) of an RS. According to the color scale, every element of an RPM shows the statistical probability of the temporal rank relationship of the two neurons among the bursts in an RS.

To quantitatively compare the RPMs of two RSs we unfolded the upper triangular parts of two RPMs into two vectors, and calculated the correlation coefficient between these vectors to represent the correlation between the two RPMs. The upper triangular part of the RPM contains the same information about the matrix as the lower triangular part. So the upper triangular part was extracted and converted into a one-dimensional vector. To do this, it was "unfolded" into a $1 \times (N(N-1)/2)$ vector V_k, row by row,

$$V_k = (p_{k21}, p_{k31}, p_{k32}, p_{k41}, p_{k42}, p_{k43}, \ldots, p_{kN1}, \ldots, p_{kN(N-1)}).$$

Operation $< V_k, V_l >= \sum_{i=2}^{N}\sum_{j=1}^{i-1} p_{kij} \cdot p_{lij}$ was defined as the inner product operation. Then the length of V_k was given by $|V_k| = \sqrt{\sum_{i=2}^{N}\sum_{j=1}^{i-1} p_{kij} \cdot p_{kij}}$, the angle between V_k and V_l was calculated as $\theta_{kl} = \arccos\frac{V_k \cdot V_l}{|V_k| \cdot |V_l|} = \arccos\frac{\sum_{i=2}^{N}\sum_{j=1}^{i-1} p_{kij} \cdot p_{lij}}{\sqrt{\sum_{i=2}^{N}\sum_{j=1}^{i-1} p_{kij} \cdot p_{kij}} \cdot \sqrt{\sum_{i=2}^{N}\sum_{j=1}^{i-1} p_{lij} \cdot p_{lij}}}$.

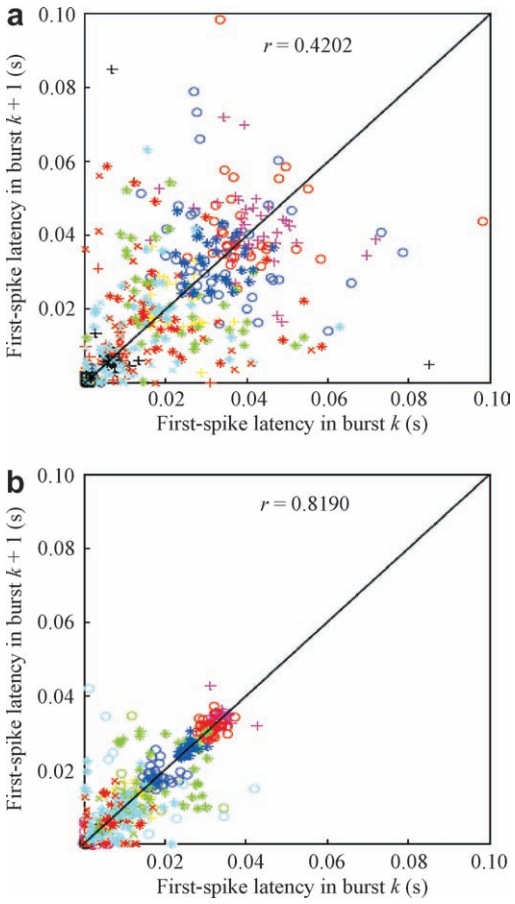

Fig. 2. Return plots representing the temporal structure of burst propagation by recursively plotting the first-spike latencies at which a neuron starts to participate in one burst against its first-spike latency in the next burst. (a) Return plots of the first-spike latencies of evoked bursts in the native state. Each type of symbol represents the first-spike latencies of one neuron. (b) Return plots of the first-spike latencies of evoked bursts in the disinhibition state. The symbols as in (a).

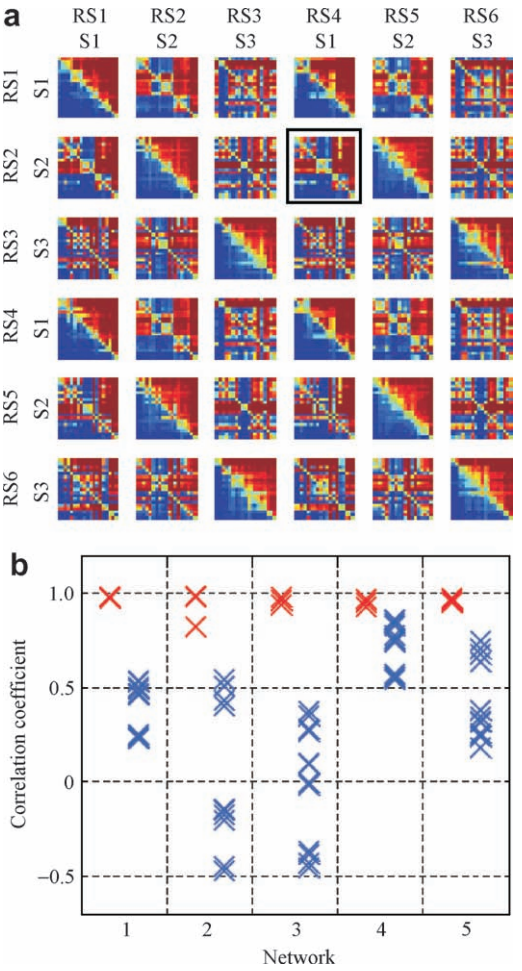

Fig. 3. (a) rRPMs of the RSs with antagonists, which contain the bursts evoked by the stimulation from S1, S2 and S3, respectively, under the condition with the antagonists. The sequence of the first-spikes in each RS is used to rearrange the RPMs into a row of rRPMs. For example, the rRPM in the black frame is an rRPM of RS4, which is rearranged according to the sequence of first-spikes of RS2. The rRPMs on the diagonal are the ones rearranged by their own sequence in each row. Different pixels represent the rank probability values of different neuron pairs using the colored scale bar. (b) For each network, correlation coefficients between the RPMs of the RSs are represented. Correlation coefficients between RSs of the same stimulation site are indicated by red crosses. Correlation coefficients between RSs of the different stimulation sites are indicated by blue crosses.

So the correlation coefficient between the RPM of RS k and the RPM of RS l was calculated as $c_{kl} = \cos\theta_{kl} = \frac{V_k \cdot V_l}{|V_k| \cdot |V_l|}$.

We then rearranged the elements of RPM using the index vector of each RS. The vector length of each row i in the RPM was obtained by $S^o_{ki} = \sqrt{p^{0}_{ki1}{}^2 + p^{0}_{ki2}{}^2 + \cdots + p^{0}_{kiN}{}^2}$, which line up together into a column vector S^o_k. Elements of S^o_k are rearranged in a descending order to get $S_k = S^o_k(I_k)$, in which I_k is the index vector of RS k, showing the order of rearranged unit numbers, and also representing the temporal order of neuronal engagement in bursts within the RS. For RS k, I_k was used

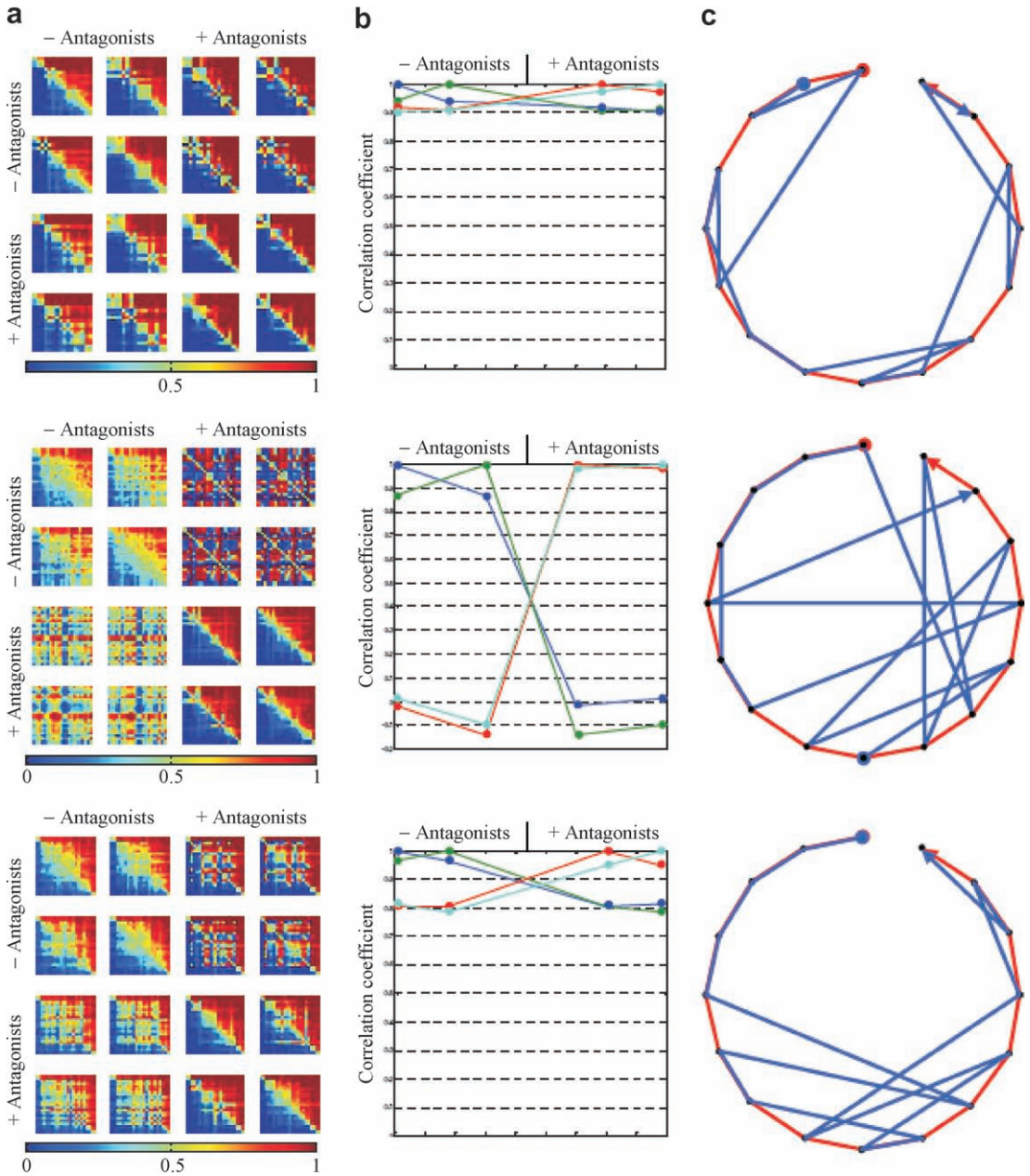

Fig. 4. (a) For each stimulation site, the joint rRPMs of evoked bursts with the antagonists and those without the antagonists were generated. The panels are drawn in the same way as Fig. 3(a), and different pixels represent the rank probability values of different neuron pairs using the colored scale bar. Each panel represents records that are made using one stimulation site, containing four RSs, in which two RSs are without the antagonists and the other two are with the antagonists. From top to bottom, the panels correspond to the stimulation sites S1, S2 and S3, respectively. (b) The correlation coefficients quantitatively represent the differences between the patterns in panel (a). They also correspond to the stimulation sites S1, S2 and S3, respectively from top to bottom. Dots represent correlation coefficients between two RSs. For example, the red dots show the correlation coefficient values between the third RS and all the RSs (including the third RS itself). (c) Each panel shows data obtained from one stimulation site, every black dot represents a recorded neuron. The neuron numbers are arranged on a circle in the temporal sequence of the first-spikes under the condition without the antagonists, and the sequence is indicated by the red lines between neurons. The temporal sequence of neurons with the antagonists is indicated by the blue lines. Under each condition, the bigger dot indicates the neuron which fires earliest, and the terminal of the arrow indicates the neuron which fires the latest. From top to bottom, the panels correspond to the stimulation sites S1, S2 and S3, respectively.

as the index to rearrange RPM P_k^0 both by rows and columns to obtain a new matrix rearranged rank-probability-matrix (rRPM) $P_k^{(I_k)}$. For another RS, RS l, according to I_k, P_l^0 was rearranged to be $P_l^{(I_k)}$. Hence, according to I_k, a series of RPMs were converted into rRPMs.

3. Results

3.1. Dynamics of the first-spike latencies in the native state and in the disinhibited state

We constructed return plots of the first-spike latencies of individual neurons between the consecutive bursts. In this way, we can examine the dynamics of the first-spike latencies. If individual neurons play conserved roles in bursts, then the first-spike latencies of an individual neuron should be conserved from burst to burst and cluster in a confined region. Moreover, the first-spike latencies of different neurons should be lined up along the diagonal of the return plot. For the native state, the first-spike latencies of different neurons were consistent across the successive bursts in some degree [$r = 0.4202$; Fig. 2(a)]. Compared with the native state, the first-spike latencies in the disinhibited state were more consistent [$r = 0.8190$; Fig. 2(b)]. Moreover, the first-spike latencies of an individual neuron cluster in a smaller confined region in the disinhibited state compared to the native state (Fig. 2). This means that individual neurons play conserved roles in bursts in the disinhibited state more strictly than in the native state. Furthermore, most of the first-spike latencies in the native state were in the range of 0–0.08 s, whereas most of the first-spike latencies in the disinhibited state were in the range of 0–0.04 s. This indicates that the propagation of bursting activities in the disinhibited state is much faster than that in the native state.

3.2. Spatiotemporal patterns of neuronal first recruitment in evoked bursts with the antagonists

The rRPMs in Fig. 3(a) represent the rank relationships between neurons of the six RSs of a network in the disinhibited state. In each row of the 6×6 format, compared with the rRPMs on the diagonal, the rank relationship patterns of the same stimulation site are strikingly similar, and the distribution of colored pixels of the rRPMs of different stimulation sites is distinctly different. Stimuli from different stimulation sites result in distinguishable patterns of neuronal rank relationships specific to the stimulation sites. Fig. 3(b) shows the correlation coefficients of RSs of five different networks. Most correlation coefficients between RSs of different sites are far below 1.0; and the correlation coefficients between RSs of the same site are near 1.0. This means that neuronal networks with disabled inhibitory synapses can be induced by the electrical stimulation to generate stable and distinguishable spatiotemporal patterns of neuronal first recruitment, and the patterns are specific to the stimulation sites.

3.3. Changes of spatiotemporal patterns of neuronal first recruitment in evoked bursts caused by the disinhibition

In this part, the data acquired in steps (1) and (2) of the experimental procedure were analyzed. In the network, for the stimulation site S1, there was little difference in the spatiotemporal patterns of evoked bursts with and without the antagonists (top panel, Fig. 4(a)); for the stimulation site S2, the spatiotemporal patterns of evoked bursts with the antagonists were distinctly different from the patterns without the antagonists (middle panel, Fig. 4(a)); for the stimulation site S3, the difference in the patterns was intermediate (bottom panel, Fig. 4(a)). The correlation coefficients (Fig. 4(b)) quantitatively represent the differences between the patterns in Fig. 4(a). According to the sequence of the first-spikes of neurons in the RSs, the spatial propagation of each stimulation site with or without the antagonists is shown in Fig. 4(c), respectively. The change of spatiotemporal patterns resulting from the blockade of inhibitory synapses is obvious.

Furthermore, based on the data from five different neuronal networks, the statistical results of correlation coefficients between evoked bursts with and without the antagonists are shown in Fig. 5. The correlation coefficients between RSs of the same stimulation site without the antagonists are all near 1.0. That goes for the correlation coefficients between RSs of the same stimulation site with the antagonists as well. The correlation coefficients between the two different conditions are dispersed in the range from −0.5 to 1.0, which are significantly less than those calcu-

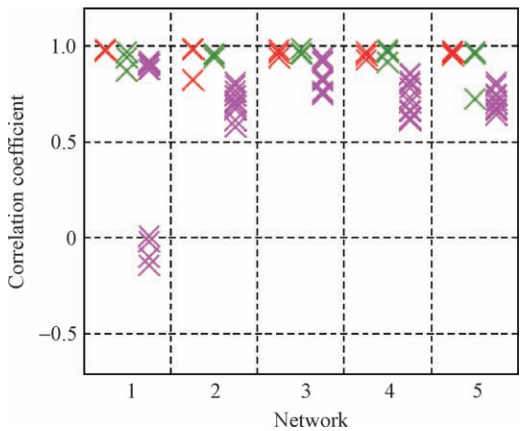

Fig. 5. The correlation coefficients between evoked bursts with and without antagonists in five different networks. The pharmacological procedure and the concentration used for each network are the same. BIC (20 μM), CGP35348 (1 μM) and STR (1 μM) were applied to block the inhibitory synapses for each network. The red crosses represent the correlation coefficients between RSs of the same stimulation site without the antagonists. The green crosses indicate the correlation coefficients between RSs of the same stimulation site with the antagonists. The purple crosses represent the correlation coefficients between the two different conditions.

lated for RSs under the same condition. The disinhibition can change the spatiotemporal patterns of neuronal first recruitment in evoked bursts in a heterogeneous manner with regard to different propagation pathways.

4. Discussion

Many *in vitro* experiments indicate that the bursting rate of networks can be substantially increased by the addition of bicuculline to the extracellular medium [11,12]. Although other studies have explored the spatiotemporal relationship of neuronal activities in networks with disabled inhibitory synapses, such studies were limited to analyzing the spread of spontaneous activity and not activities triggered by an electrical stimulus [7,15]. The effects of bicuculline on the network activity evoked by an electrical stimulation were studied by several groups. Eytan et al. found that increased responsiveness to rarely stimulated sites depended specifically on fast GABAergic transmission and they concluded that the inhibitory sub-network, excitatory synaptic depression, and their balance all play active roles in generating selective gain control [10]. Yvon et al. have also shown that bursts can be triggered by an external electrical stimulation in disinhibited cultures, and they also analyzed the factors affecting the success of stimulation [16]. Li et al. have shown that the inhibitory connection degrades in an age-dependent manner in the development of the networks *in vitro* of dissociated neurons from an embryonic rat hippocampus [17]. Yet, none of these reports address the effect of BIC on the spatiotemporal patterns of evoked activity.

To recapitulate, in the present study, we analyzed precise timing of the first-spikes and constructed return plots to show the timing dynamics of the first-spikes caused by disinhibition. This analysis showed that, compared with the native state, the first-spike latencies in the disinhibited state are more consistent. In addition, we found that the propagation of the bursting activities in the disinhibited state is much faster than that in the native state. Furthermore, we analyzed rank relationships between first-spikes, and represented the spatiotemporal patterns of neuronal first recruitment in bursts as rRPMs, and calculated the correlation coefficients between the rRPMs. This analysis clearly illustrated the differences of spatiotemporal patterns between evoked bursts of different stimulation sites. The disinhibited neuronal networks could be induced by the electrical stimulation to generate stable and distinguishable spatiotemporal patterns of neuronal first recruitment, and the patterns were specific to the stimulation sites. This indicates that excitatory synaptic transmission is necessary and also sufficient for the initiation and spread of activity in a network.

To account for why disinhibition may cause the original spatiotemporal patterns to change in a heterogeneous manner, we note that each propagation pathway is composed of many excitatory and inhibitory synapses. The number, efficiency and positions of inhibitory synapses involved in may vary, causing differences in the extent of inhibitory synaptic contribution, with different stimulation sites evoking different pathways. As such, when inhibitory activity is suppressed, different pathways are affected to different extents, causing heterogeneous changes in the original spatiotemporal patterns.

Acknowledgements

This work was supported by the National High-Tech Research and Development Program of China (Grant No. 2006AA020701). We thank Mr. Andy Wong for critically reading the manuscript.

References

[1] Beggs JM, Plenz D. Neuronal avalanches in neocortical circuits. J Neurosci 2003;23:11167–77.
[2] Beggs JM, Plenz D. Neuronal avalanches are diverse and precise activity patterns that are stable for many hours in cortical slice cultures. J Neurosci 2004;24:5216–29.
[3] Darbon P, Scicluna L, Tscherter A, et al. Mechanisms controlling bursting activity induced by disinhibition in spinal cord networks. Eur J Neurosci 2002;15:671–83.
[4] Izhikevich EM, Gally JA, Edelman GM. Spike-timing dynamics of neuronal groups. Cereb Cortex 2004;14:933–44.
[5] Maeda E, Robinson HPC, Kawana A. The mechanisms generation and propagation of synchronized bursting in developing networks of cortical neurons. J Neurosci 1995;15:6834–45.
[6] Segev R, Baruchi I, Hulata E, et al. Hidden neuronal correlations in cultured networks. Phys Rev Lett 2004;92:118102.
[7] Streit J, Tscherter A, Heuschke MO, et al. The generation of rhythmic activity in dissociated cultures of rat spinal cord. Eur J Neurosci 2001;14:191–202.
[8] Volmana V, Baruchia I, Persia E, et al. Generative modelling of regulated dynamical behavior in cultured neuronal networks. Physica A 2004;335:249–78.
[9] Wagenaar DA, Nadasdy Z, Potter SM. Persistent dynamic attractors in activity of patterns of cultured neuronal networks. Phys Rev E 2006;73:051907.
[10] Eytan D, Brenner N, Marom S. Selective adaptation in networks of cortical neurons. J Neurosci 2003;23:9349–56.
[11] Jimbo Y, Kawana A, Parodi P, et al. The dynamics of a neuronal culture of dissociated cortical neurons of neonatal rats. Biol Cybern 2000;83:1–20.
[12] Morefield SI, Keefer EW, Chapman KD, et al. Drug evaluations using neuronal networks cultured on microelectrode arrays. Biosens Bioelectron 2000;15:383–96.
[13] Xiang G, Pan L, Huang L, et al. Microelectrode array-based system for neuropharmacological applications with cortical neurons cultured in vitro. Biosens Bioelectron 2007;22:2478–84.
[14] Shoham S, Fellows MR, Normann RA. Robust, automatic spike sorting using mixtures of multivariate t-distributions. J Neurosci Methods 2003;127:111–22.
[15] Whittington MA, Traub RD. Interneuron diversity series: inhibitory interneurons and network oscillations in vitro. Trends Neurosci 2003;26:676–82.
[16] Yvon C, Rubli R, Streit J. Patterns of spontaneous activity in unstructured and minimally structured spinal networks in culture. Exp Brain Res 2005;165:139–51.
[17] Li X, Zhou W, Zeng S, et al. Long-term recording on multi-electrode array reveals degraded inhibitory connection in neuronal network development. Biosens Bioelectron 2007;22:1538–43.